JCMM
Available online at
www.jcmm.ro
www.jcmm.org

J. Cell. Mol. Med. Vol 10, No 1, 2006 pp. 243-257

In Focus

Interstitial Cajal-like cells (ICLC) in atrial myocardium: ultrastructural and immunohistochemical characterization

M.E. Hinescu [a,b], Mihaela Gherghiceanu [b], E. Mandache [b], Sanda M. Ciontea [a], L.M. Popescu [a,b] *

[a] *Department of Cellular and Molecular Medicine, 'Carol Davila' University of Medicine and Pharmacy, Bucharest, Romania*
[b] *'Victor Babes' National Institute of Pathology, Bucharest, Romania*

Received: January 15, 2006; Accepted: February 27, 2006

Abstract

We have previously reported (Hinescu & Popescu, 2005) the existence of interstitial Cajal-like cells (ICLC), by transmission electron microscopy, in human atrial myocardium. In the present study, ICLC were identified with non-conventional light microscopy (NCLM) on semi-thin sections stained with toluidine blue and immunohistochemistry (IHC) for CD117/c-kit, CD34, vimentin and other additional antigens for differential diagnosis. Quantitatively, on semi-thin sections, ICLC represent about 1–1.5% of the atrial myocardial volume (*vs.* ~45% working myocytes, ~2% endothelial cells, 3–4% for other interstitial cells, and the remaining percentage: extracellular matrix). Roughly, there is one ICLC for 8–10 working atrial myocytes in the intercellular space, beneath the epicardium, with a characteristic (pyriform, spindle or triangular) shape. These ICLC usually have 2–3 definitory processes, emerging from cell body, which usually embrace atrial myocytes (260 nm average distance plasmalemma/sarcolemma) or establish close contact with nerve fibers or capillaries (~420 nm average distance to endothelial cells). Cell prolongations are characteristic: very thin (mean thickness = 0.150±0.1 μm), very long for a non-nervous cell (several tens of μm) and moniliform (uneven caliber). Stromal synapses between ICLC and other interstitial cells (macrophages) were found (*e.g.* in a *multicontact* type synapse, the average synaptic cleft was ~65 nm). Naturally, the usual cell organelles (mitochondria, smooth and rough endoplasmic reticulum, intermediate filaments) are relatively well developed. Caveolae were also visible on cell prolongations. No thick filaments were detected. IHC showed that ICLC were slightly and inconsistently positive for *CD117/c-kit*, variously co-expressed *CD34* and *EGF receptor*, but appeared strongly positive for *vimentin*, along their prolongations. Some ICLC seemed positive for *α-smooth muscle actin* and *tau protein*, but were negative for *nestin*, *desmin*, *CD13* and *S-100*.

In conclusion, we provide further evidence of the existence of ICLC in human atrial myocardium, supporting the possible ICLC role in pacemaking, secretion (juxta- and/or paracrine), intercellular signaling (neurons and myocytes). For pathology, ICLC might as well be 'players' in arrhythmogenesis and atrial remodeling.

Keywords: interstitial Cajal-like cells • human atrial myocardium • CD117/c-kit • CD34 • vimentin • stromal synapse • intercellular signaling • EGF-receptor • CD13 • desmin • electron microscopy

Introduction

At present, the ultrastructural [1–3], immunocytochemical [4, 5] and electrophysiological [6–8] properties of interstitial cells of Cajal (ICC) from the intestinal tract are 'sufficiently' known and the corresponding literature extensively reviewed.

Therefore, naturally, a question arised: are interstitial Cajal-like cells located outside the gut musculature ? [9]. The answer was positive for several cases, *e.g.*: vasculature [10, 11]; exocrine pancreas

* Correspondence to: L.M. POPESCU, M.D., Ph.D.
Department of Cellular and Molecular Medicine,
"Carol Davila" University of Medicine and Pharmacy,
P.O. Box 35-29, Bucharest 35, Romania.
E-mail: LMP@univermed-cdgm.ro
LMP@jcmm.org

Reprinted from:
Journal of Cellular and Molecular Medicine

Published by:
the CMM Foundation

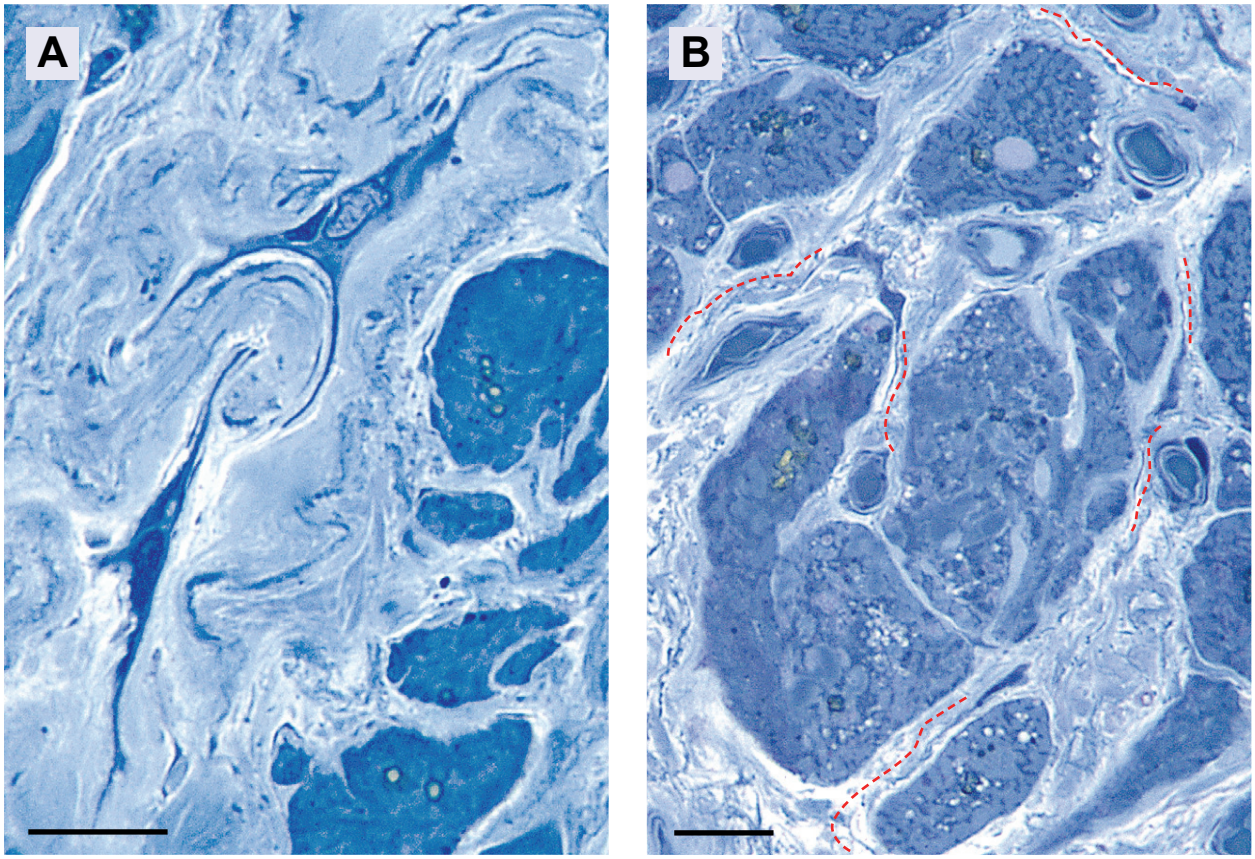

Fig. 1 A–F Human atrial myocardium. Representative light microscopic images of semi-thin sections of Epon-embedded material stained with toluidine blue. Note the atrial ICLC with very long, thin processes, delineated by red dotted lines, and disposed around the working cardiomyocytes (oblique and cross sections **A**–**D** and longitudinally-cut in **E**, **F**). The punctate brown staining corresponds to lipofuscin pigment granules. Scale bars = 10μm.

[12]; female [13–15] or male [16, 17] reproductive tract; upper [18] or lower [19–21] urinary tract; mammary gland [22], etc. Moreover, besides the well-known gastrointestinal stromal tumors (so-called GISTs), which start from ICC, extra-GISTs are now considered a new pathological entity, originating probably from ICLC [23].

Our working hypothesis was that ICLC could exist in the interstitium of atrial myocardium. Indeed, we previously presented electron microscope images, strongly suggesting that ICLC could be identified in human atrial myocardium [24]. This might be surprising for many electron microscopists, because the trivial belief is not very far from the following: '...despite electron microscopy having been used for a considerable time relatively few cases appeared to benefit directly from this investigation' [25].

Myocardial interstitium was mostly overlooked, since, on the one hand, people were focused on muscle cells and their atrial granules, or, on the other hand, the ultrastructure of the interstitial space seems rather monotonous. In this context, it was hard to believe for morphologists that a novel cell type could still exist in the myocardium.

In the heart, fibroblasts form one of the largest cell populations, in terms of cell numbers [26, 27], and most recent studies point out their structural and functional heterogeneity [28]. Therefore, ICLC, that share common features with some ‘classical’ fibroblasts, might be in fact a subpopulation of the atrial interstitial cells, taken *in toto* as ‘fibroblasts’.

We present here correlated morphological, ultrastructural and immunocytochemical data that confirm the presence of ICLC in human and rat atrial myocardium.

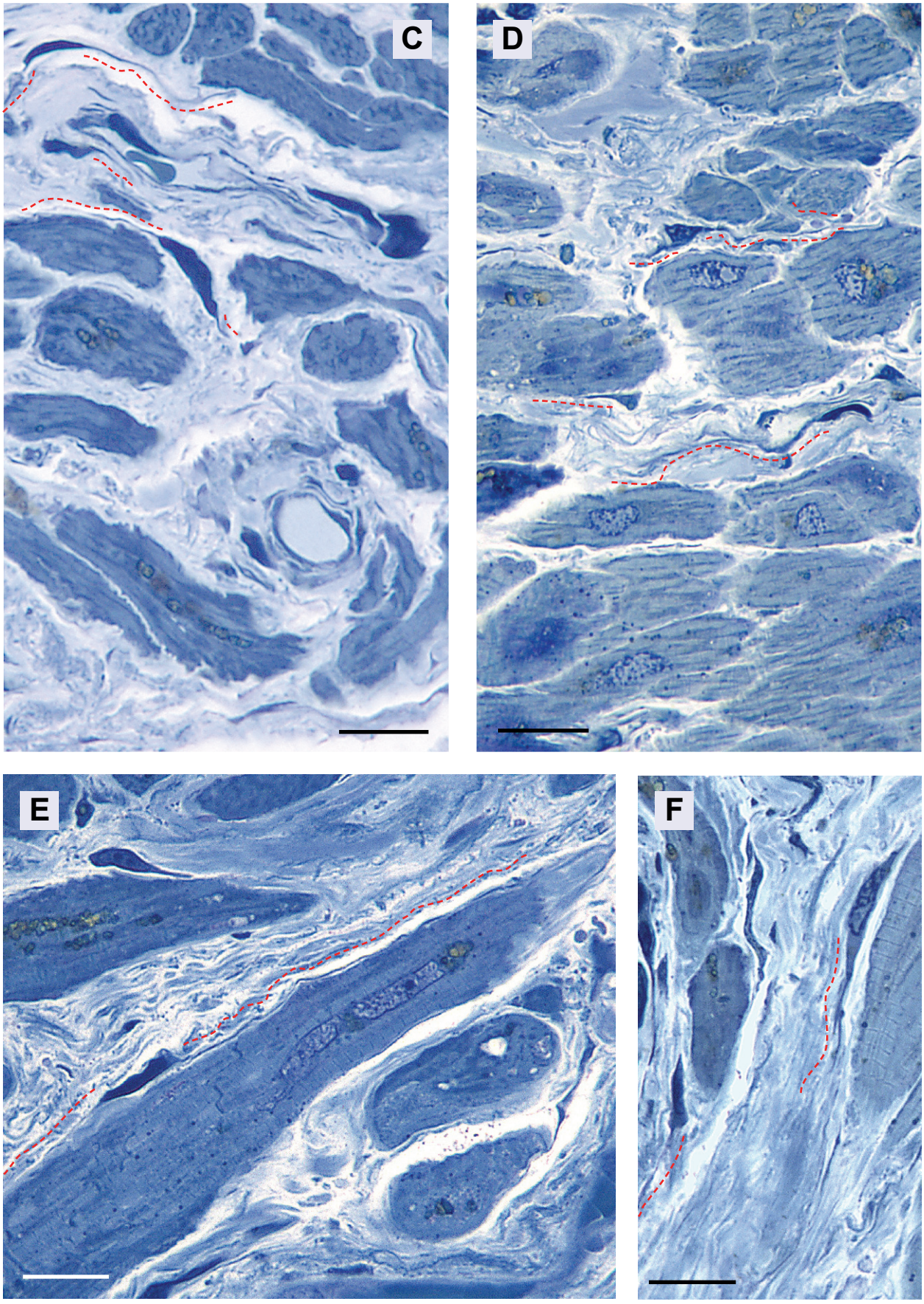
C
D
E
F

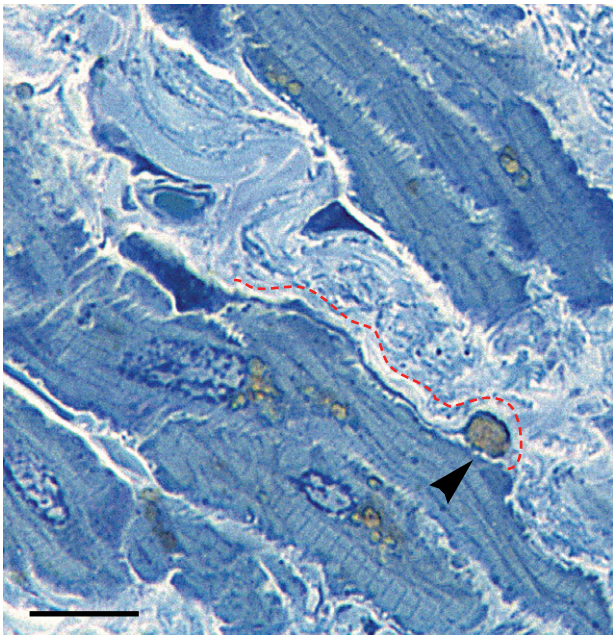

Fig. 2 Human right atrial myocardium. Semi-thin section of Epon-embedded material stained with toluidine blue. An ICLC body with a very long emerging cytoplasmic process can be easily recognized. Its ending surrounds some extracellular lipid material (possibly lipofuscin pigment granules; arrowhead). Scale bar = 10μm.

Material and methods

Human tissue samples

The study was performed on archived atrial Epon-embedded tissue specimens, obtained with written consent from patients undergoing cardiac surgery. This study was approved by the Bioethics Committee of the 'Carol Davila' University of Medicine and Pharmacy, Bucharest, according to generally accepted international standards. Tissue specimens (about 1 mm^3) were fixed in 4% glutaraldehyde in 0.1 M cacodylate buffer, pH 7.3, for 4 h, at 4°C. After a brief wash in 0.1 M cacodylate buffer, tissue samples were post-fixed with 1% osmium tetroxide in same buffer, pH 7.3, at 4°C, followed by dehydration in a graded series of ethanols. After impregnation in propylene oxide, the samples were immersed overnight in a mixture of propylene oxide and Epon 812 resin, and embedded in Epon 812 as usually. Ultrathin sections were cut using on MT-7000 ultramicrotome using diamond knife (Research Manufacturing Company Inc., Tucson, AZ, USA). Sections (50 nm) were collected on Formvar-coated copper grids, stained with uranyl acetate and lead citrate, and observed in a CM 12 Philips electron microscope, at an acceleration voltage of 60 kV. The quantitative evaluation

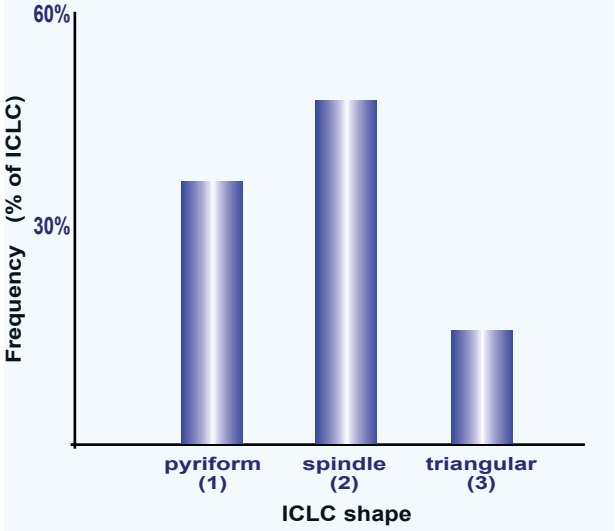

Fig. 3 Histogram showing percentile distribution of the number of cytoplasmic processes expanding from ICLC body. Cells were counted on semi-thin sections of atrial myocardium. Eighty-eight ICLC were counted, on 32 photographs.

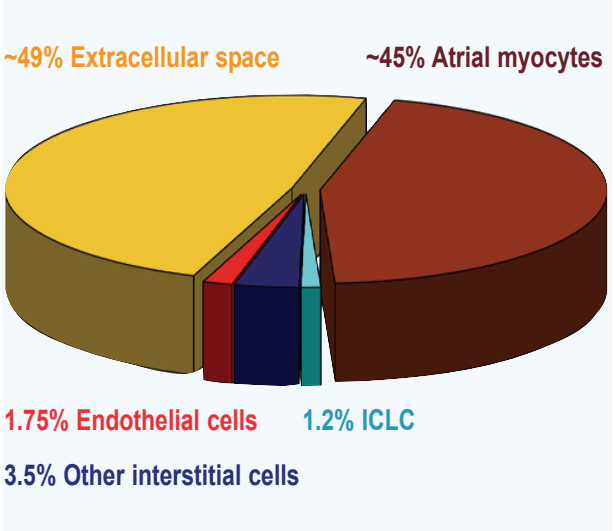

Fig. 4 Chart representing relative volumes the of human atrial tissue components. Actually, the values were: 48.6±2.5% extracellular space, 44.9±2.9% atrial myocytes. ICLC were 1.2±0.3% of total human atrial myocardial volume. Twenty-four randomly taken photographs of semi-thin sections were analysed. Values are expressed as mean ± standard error.

Fig. 5 A–C Electron microscope images showing interstitial Cajal-like cells (ICLC) from human atrial interstitium; photographic reconstructions. The profile of ICLC seems different depending on section orientation: more sinuous in cross sections (**A**, **B**) and almost linear in longitudinal section (**C**). Some cell processes surround their 'own' myocardial cell bundle while others lie between several bundles. Note in **C**, at higher magnification, two ICLC thin processes. The lack of T-tubules, an ultrastructural characteristic feature for atrial working myocytes is evident.
arrows = thin prolongations of ICLC process towards the myocyte; arrowheads = atrial granules, ultrastructural marker for atrial myocytes, m = mitochondria, rER = rough endoplasmic reticulum, Z = Z line, gly = glycogen. Scale bars = 1µm.

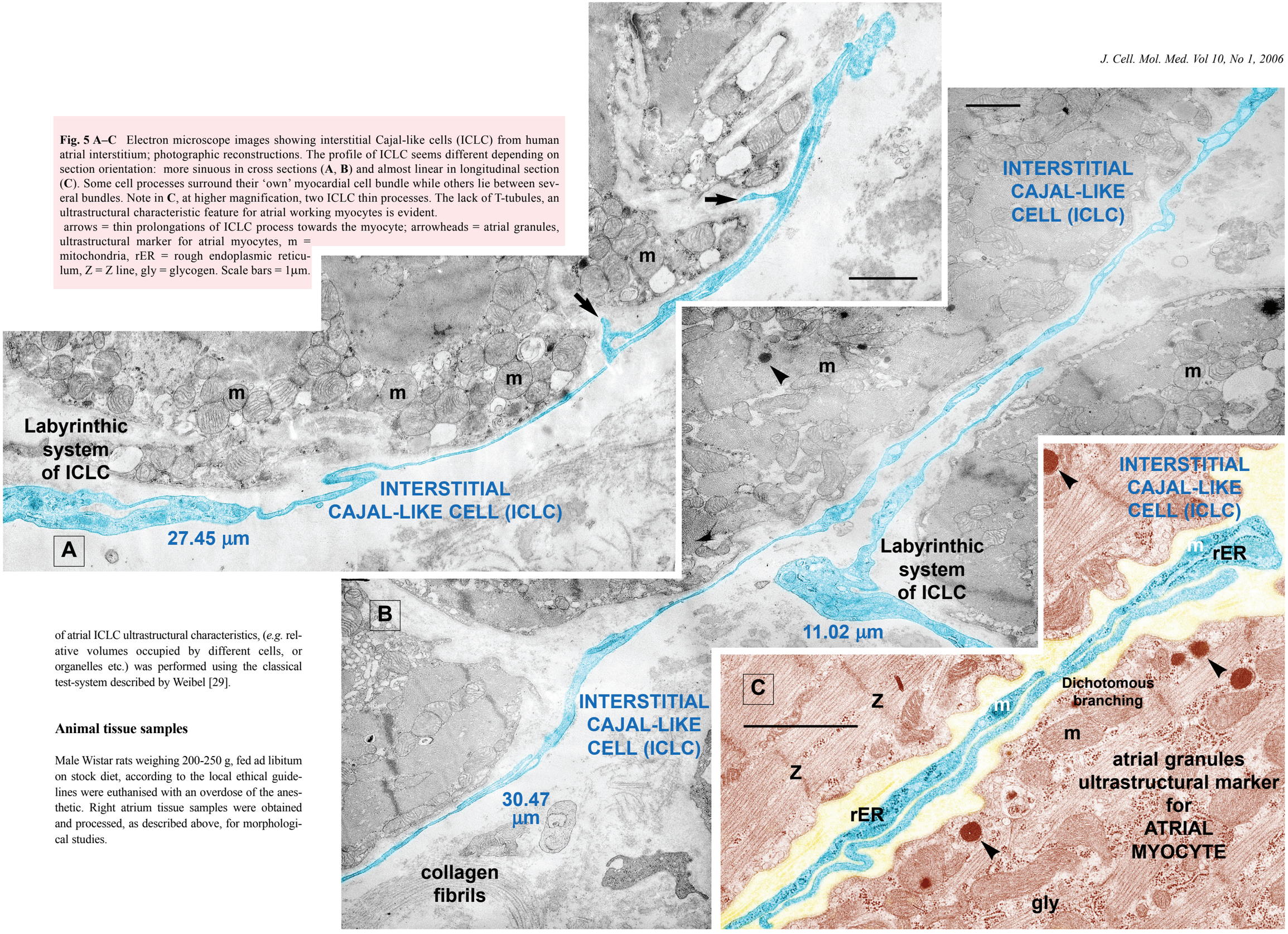

of atrial ICLC ultrastructural characteristics, (*e.g.* relative volumes occupied by different cells, or organelles etc.) was performed using the classical test-system described by Weibel [29].

Animal tissue samples

Male Wistar rats weighing 200-250 g, fed ad libitum on stock diet, according to the local ethical guidelines were euthanised with an overdose of the anesthetic. Right atrium tissue samples were obtained and processed, as described above, for morphological studies.

Fig. 6 Human atrial myocardium, oblique section. TEM (photographic reconstruction) illustrating the close vicinity of a long thin process belonging to an interstitial Cajal-like cell (ICLC), with an atrial myocyte. Note the presence of at least 20 atrial granules (arrowheads) in the central region of the cell, as well as accumulated lipofuscin (aging pigment).
m = mitochondria. Scale bar = 1µm.

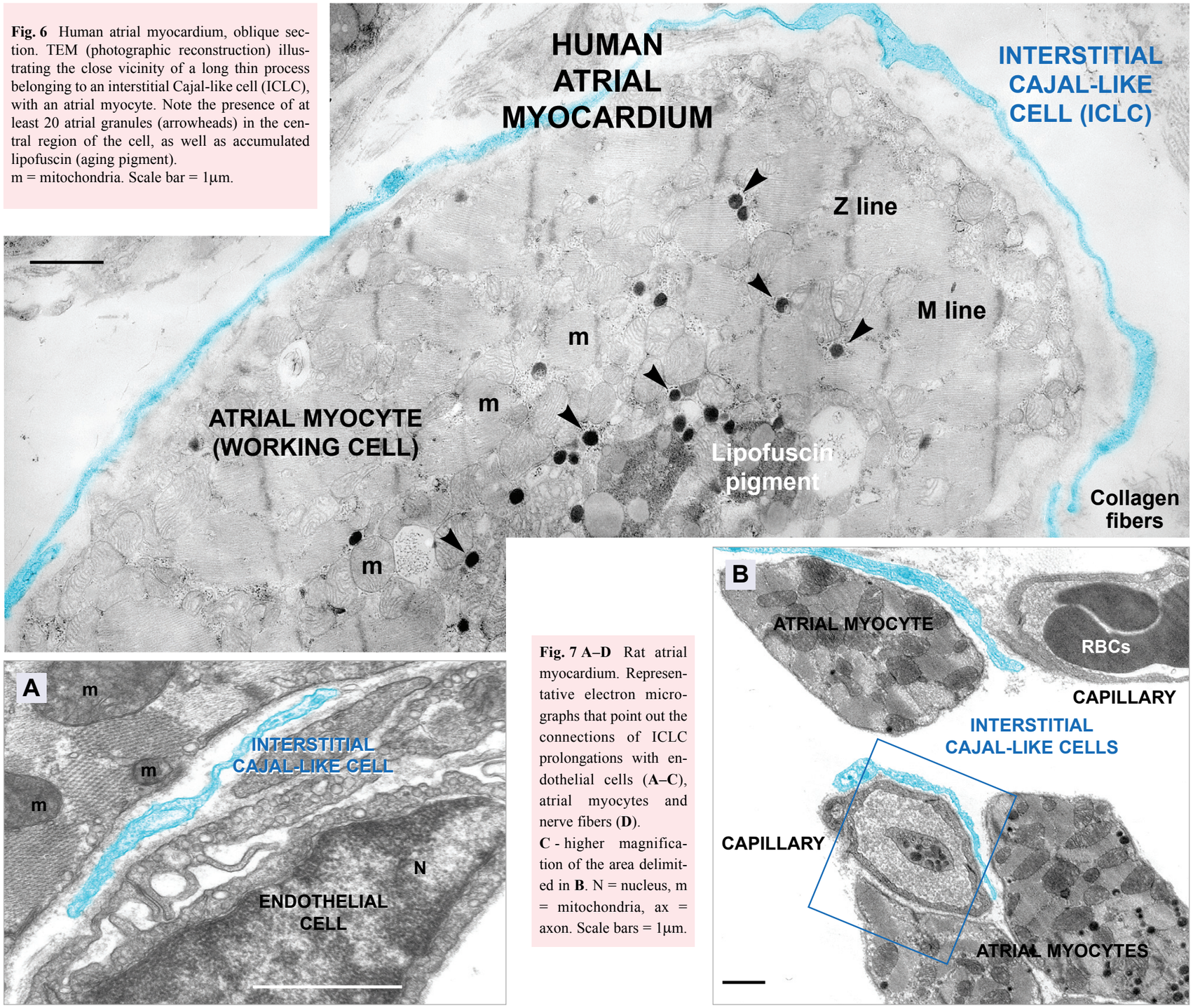

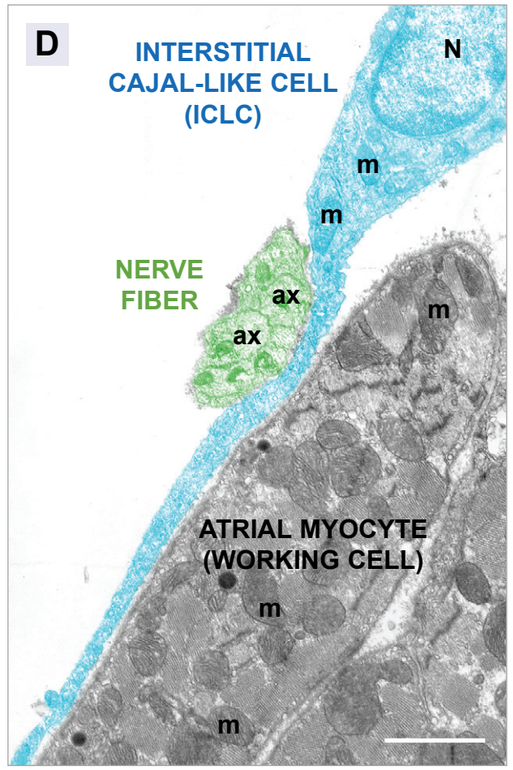

Fig. 7 A–D Rat atrial myocardium. Representative electron micrographs that point out the connections of ICLC prolongations with endothelial cells (**A–C**), atrial myocytes and nerve fibers (**D**).
C - higher magnification of the area delimited in **B**. N = nucleus, m = mitochondria, ax = axon. Scale bars = 1µm.

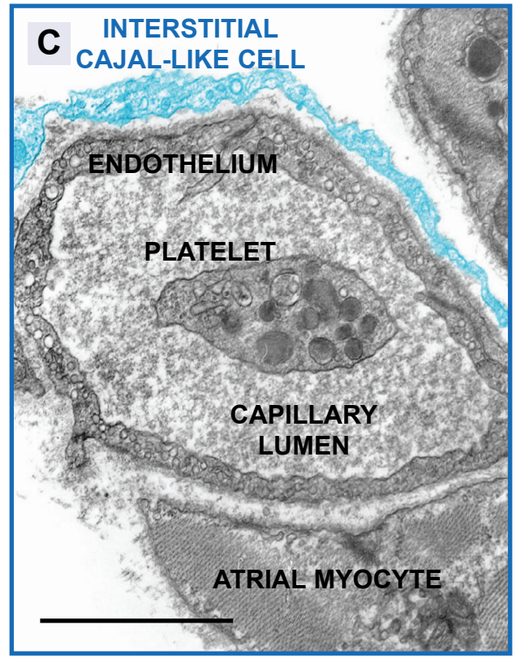

Fig. 8 A–D Rat atrial myocardium. **A**, **B.** Note the closeness of a ICLC processes (blue) with the cross-sectioned muscle cells. **C**, **D.** ICLC relationship with target structures: an intermediate position of ICLC prolongation between capillary (endothelial cell) and working cardiomyocyte (**C**); nerve fibers (axons; ax), embedded in a Schwann cell, are covered by an ICLC process, which almost adheres to them (**D**).
m = mitochondria; ax = axons;
Scale bars = 1 μm.

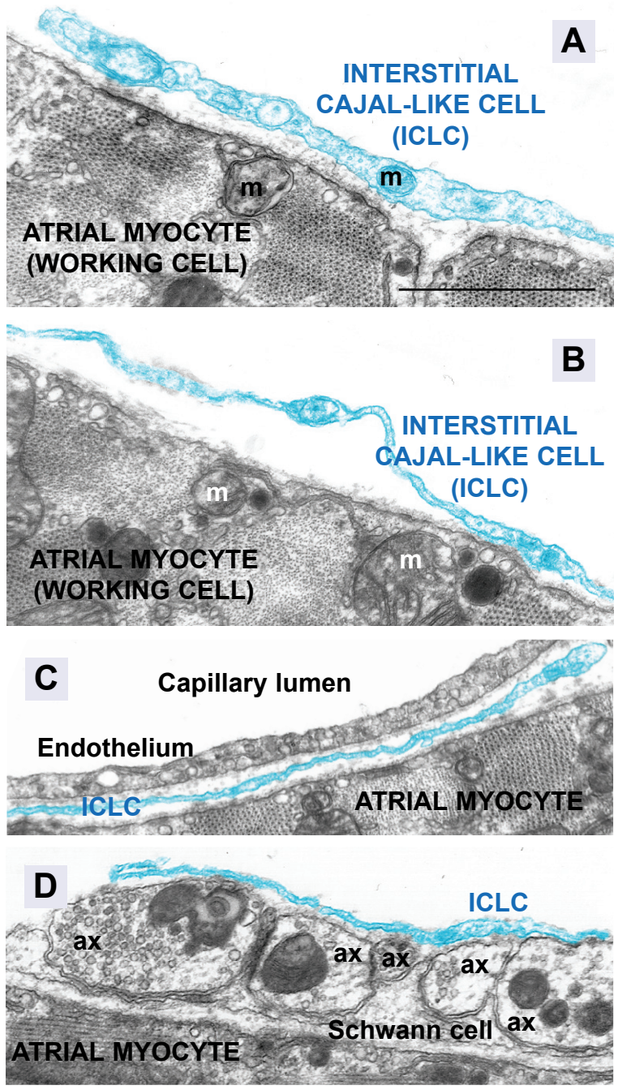

Non-conventional light microscopy (NCLM)

Control semi-thin sections (less than 1 μm) were stained with 0.25% toluidine blue and examined by light microscopy (Nikon Eclipse E600). Representative photomicrographs were taken using Nikon Plan 40x and Nikon Plan Fluor 100x/1.30 oil.

Morphometric analysis

NCLM. Twenty-four randomly taken images were analysed to determine the relative volume occupied by ICLC. Volumes were expressed as percentage, using superimposed Weibel grids [29]. ICLC number and morphology was evaluated on 32 photomicrographs (~700 cells were counted). Data were processed and statistically analysed using Microsoft Excel software.

TEM. Detailed quantitative analysis of size and length of ICLC prolongations, as well as distances to targets (or stromal synapse nanoscopy) was performed on TEM images with known magnifications, using NIH ImageJ software, after proper calibration. Statistical analysis of these parameters was also performed using ImageJ.

Immunohistochemistry (IHC)

IHC was performed on formalin-fixed, paraffin-embedded tissue sections by the avidin-biotin peroxidase complex method [30, 31]. The primary antibodies used were as follows: **CD117/c-kit**, polyclonal, 1:100 (DAKO, Glostrup, Denmark), **CD34**, monoclonal, 1: 100, clone QBEND10

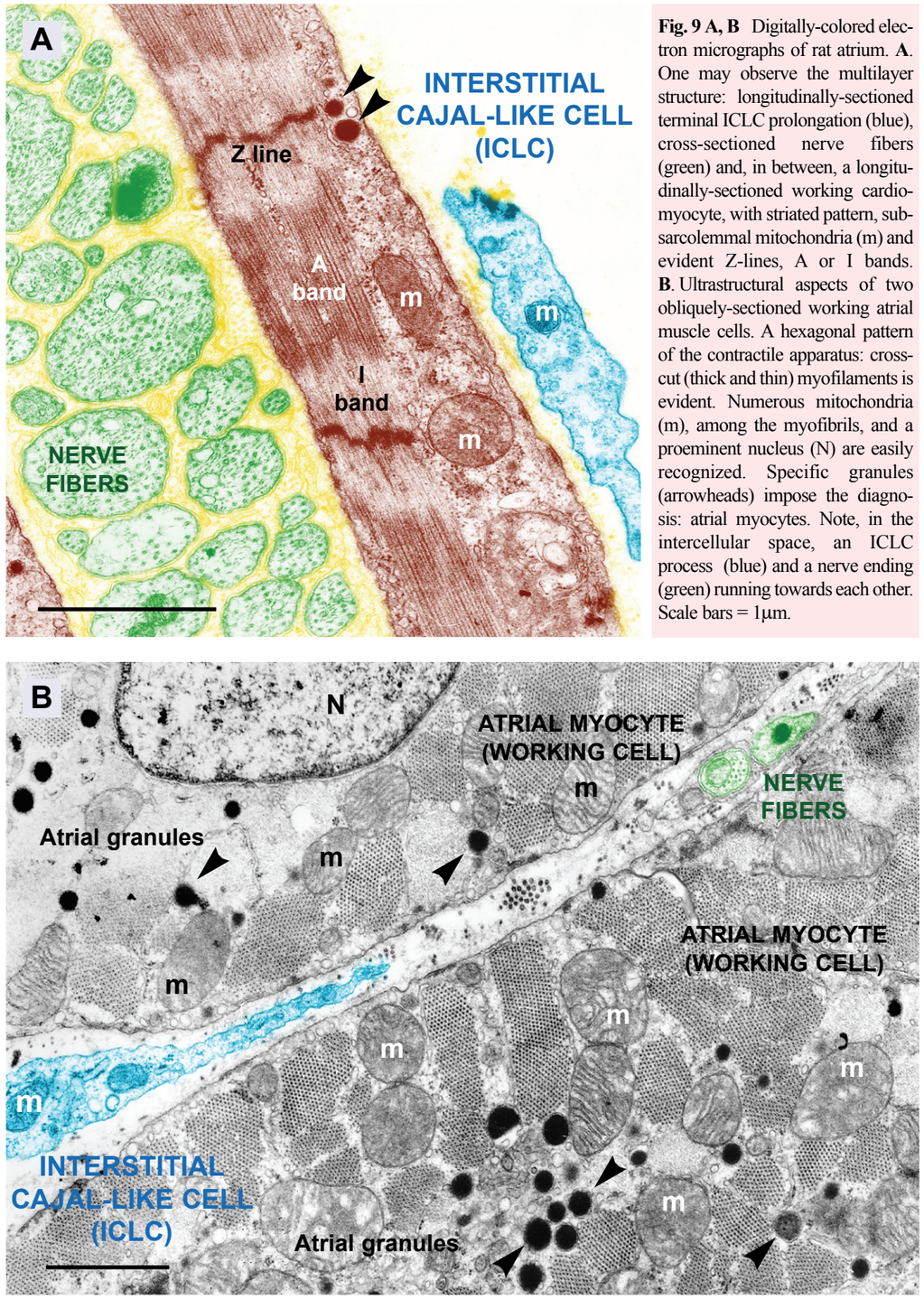

Fig. 9 A, B Digitally-colored electron micrographs of rat atrium. **A**. One may observe the multilayer structure: longitudinally-sectioned terminal ICLC prolongation (blue), cross-sectioned nerve fibers (green) and, in between, a longitudinally-sectioned working cardiomyocyte, with striated pattern, subsarcolemmal mitochondria (m) and evident Z-lines, A or I bands. **B**. Ultrastructural aspects of two obliquely-sectioned working atrial muscle cells. A hexagonal pattern of the contractile apparatus: cross-cut (thick and thin) myofilaments is evident. Numerous mitochondria (m), among the myofibrils, and a proeminent nucleus (N) are easily recognized. Specific granules (arrowheads) impose the diagnosis: atrial myocytes. Note, in the intercellular space, an ICLC process (blue) and a nerve ending (green) running towards each other. Scale bars = 1μm.

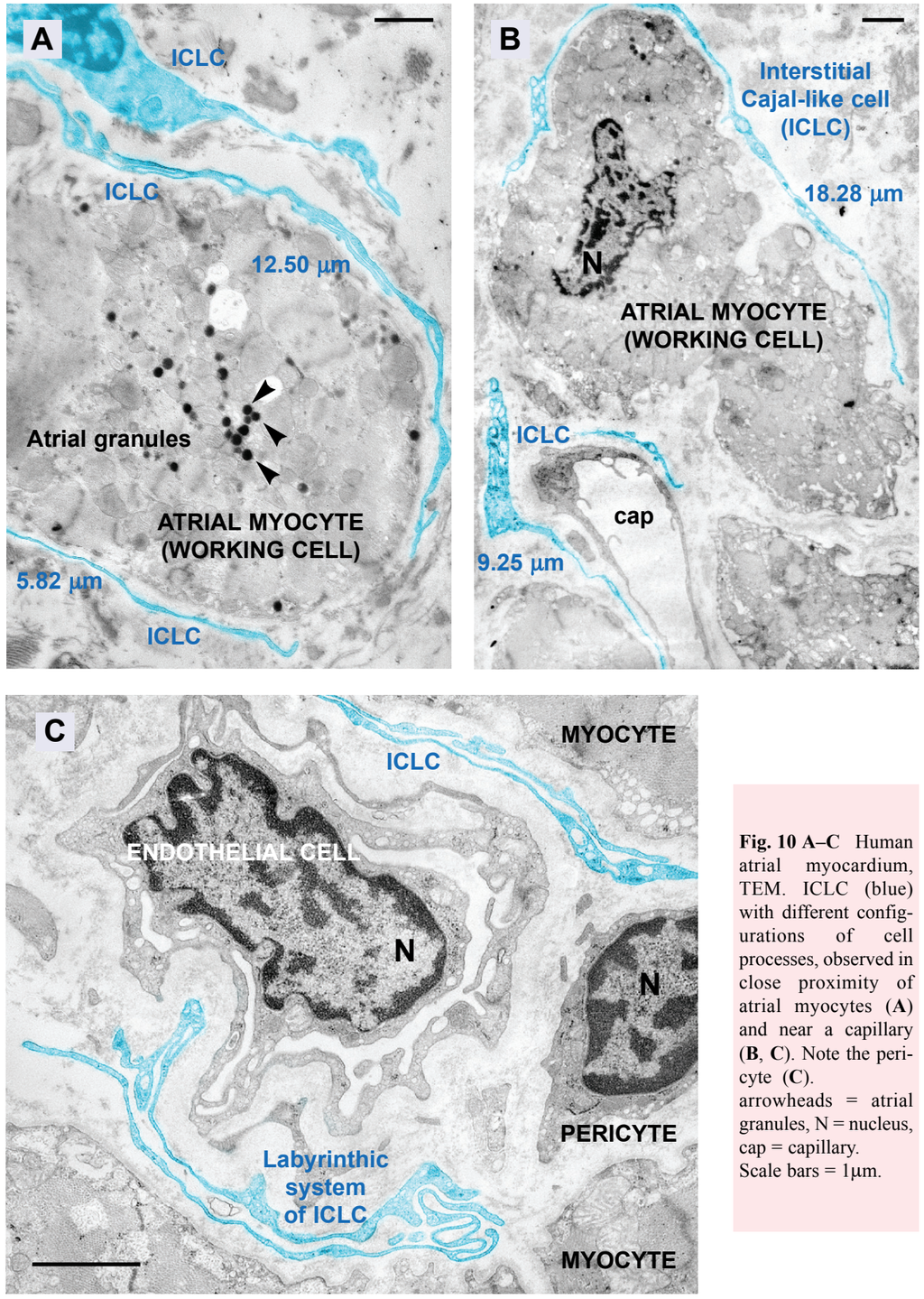

Fig. 10 A–C Human atrial myocardium, TEM. ICLC (blue) with different configurations of cell processes, observed in close proximity of atrial myocytes (**A**) and near a capillary (**B**, **C**). Note the pericyte (**C**).
arrowheads = atrial granules, N = nucleus, cap = capillary.
Scale bars = 1µm.

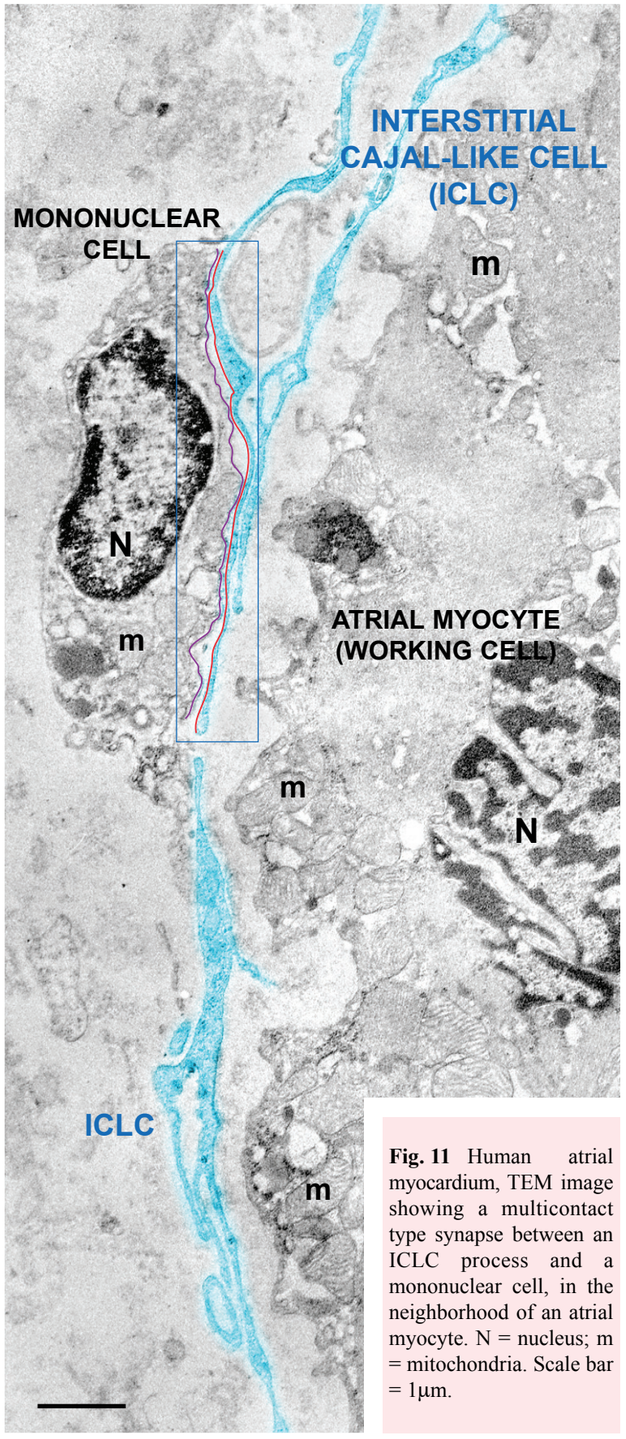

Fig. 11 Human atrial myocardium, TEM image showing a multicontact type synapse between an ICLC process and a mononuclear cell, in the neighborhood of an atrial myocyte. N = nucleus; m = mitochondria. Scale bar = 1µm.

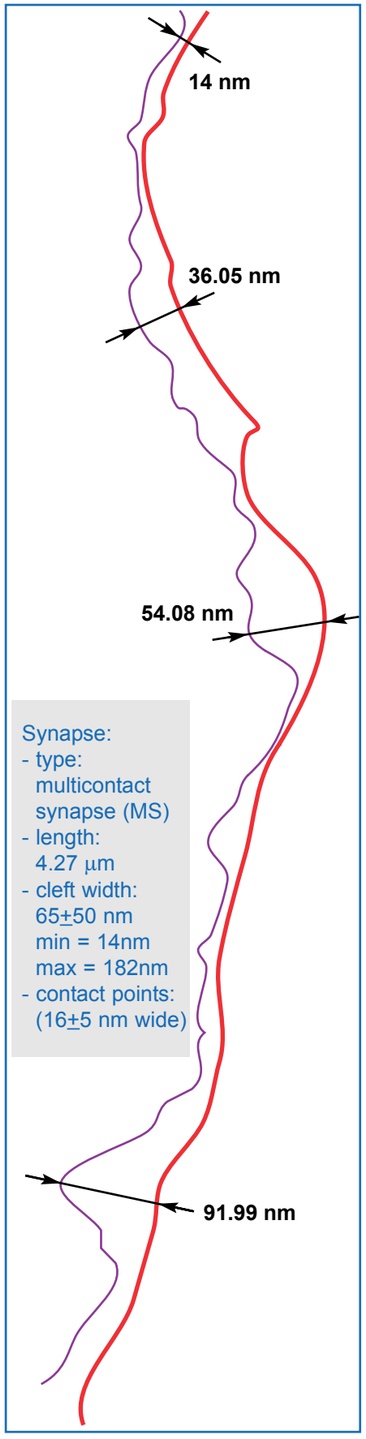

Table 1. Examples of electron microscope figures appeared in scientific papers during the last 40 years: such images contain cellular 'fragments' (particularly prolongations) suggestive for ICLC. However, this is no more than our impression. The information in this table should **not** be considered as exhaustive; it is only a routine search of the scientific literature.

Year	Author(s)	Illustration	Animal/Tissue	Original comment, if any on putative 'ICLC'	Reference
1964	Jamieson & Palade	Fig. 5	Rat atrium	No	[35]
1965	Napolitano	Figs. 1&4	Dog atrium	Cell processes	[36]
1968	James & Sherf	Fig. 4	Human (postmortem) A-V node	No	[37]
1969	McNutt & Fawcett	Fig. 7	Cat atrium	No	[38]
1972	Purdy	Fig. 3	'Synthetic' strands of embryonic chick heart	Fibroblast-like cells with long cytoplasmic processes	[39]
1973	Viragh & Challice	Fig. 31	Mouse atrial surface (9 day embryo)	Extremely flattened cell processes	[40]
1973	Legato	Fig. 1	Human atrium	No	[41]
1974	Denoit-Mazet	Fig. 5	Frog atrium	No	[42]
1974	Van der Zypen	Fig. 9	Rat interatrial septum	No	[43]
1979	Nishi	Figs. 4, 7	Rabbit atrium	No	[44]
1988	Forsmann	Fig. 26	Atrium (species not mentioned)	No	[45]
2000	Schramm	Figs. 2&4	Human atrium	No	[46]
2004	Rasmussen	Fig. 3A	Rat left atrium	No	[47]

(Biogenex, San Ramon, CA, USA), **EGF-R**, monoclonal, 1:1000, clone 29.1 (Sigma, St. Louis, MO, USA), **vimentin**, monoclonal, 1:100, clone V-9 (BioGenex, San Ramon, CA, USA), **smooth muscle α-actin** (SMA), monoclonal, 1:1500, clone 1A4 (Sigma Chemical, St. Louis, MO, USA), **tau** protein, polyclonal, 1:100 (NeoMarker, Fremont, CA, USA), **nestin**, monoclonal, 1:100, clone 5326 (Santa Cruz, CA, USA), **desmin**, monoclonal, 1:50, clone D33 (Dako, Glostrup, Denmark), **CD13**, monoclonal, 1:40, clone 38C12 (Novocastra, Newcastle upon Tyne, UK), **S-100**, polyclonal, 1:500 (DAKO, Glostrup, Denmark).

Atrial interstitial-cell isolation protocol

Male Wistar rat (4 weeks) was killed by cervical dislocation. The heart was removed and immediately placed in Dulbecco's Modified Eagle's Medium (DMEM),then dissected and repeatedly washed with DMEM supplemented with 100 UI/ml penicillin, 0.1 mg/ml streptomycin, and 0.25 μg/ml amphotericin (Sigma Chemical, St.Louis, MO, USA). After mechanical removal of pericardium and endocardium, the remaining atrial tissue was minced in fragments of about 1 mm^3, rinsed and incubated on an orbital shaker for 4 h, at 37°C, with 1 mg/ml collagenase type Ia (Sigma Chemical, St.Louis, MO, USA) in PBS. Dispersed cells were separated from non-digested tissue by filtration through a 40 μm diameter cell strainer (BD Labware, San Jose, CA, USA), collected by centrifugation at 250g, and resuspended in a 1:1 DMEM:Ham's Nutrient F-12 mixture, supplemented with 10% fetal calf serum, 1.5 mM HEPES, 100 UI/ml penicillin, 0.1 mg/ml streptomycin and 0.25 μg/ml amphotericin. Cell density was counted in a haemocytometer and viability was assessed using the Trypan blue exclusion test. Cells were distributed on glass coverslips

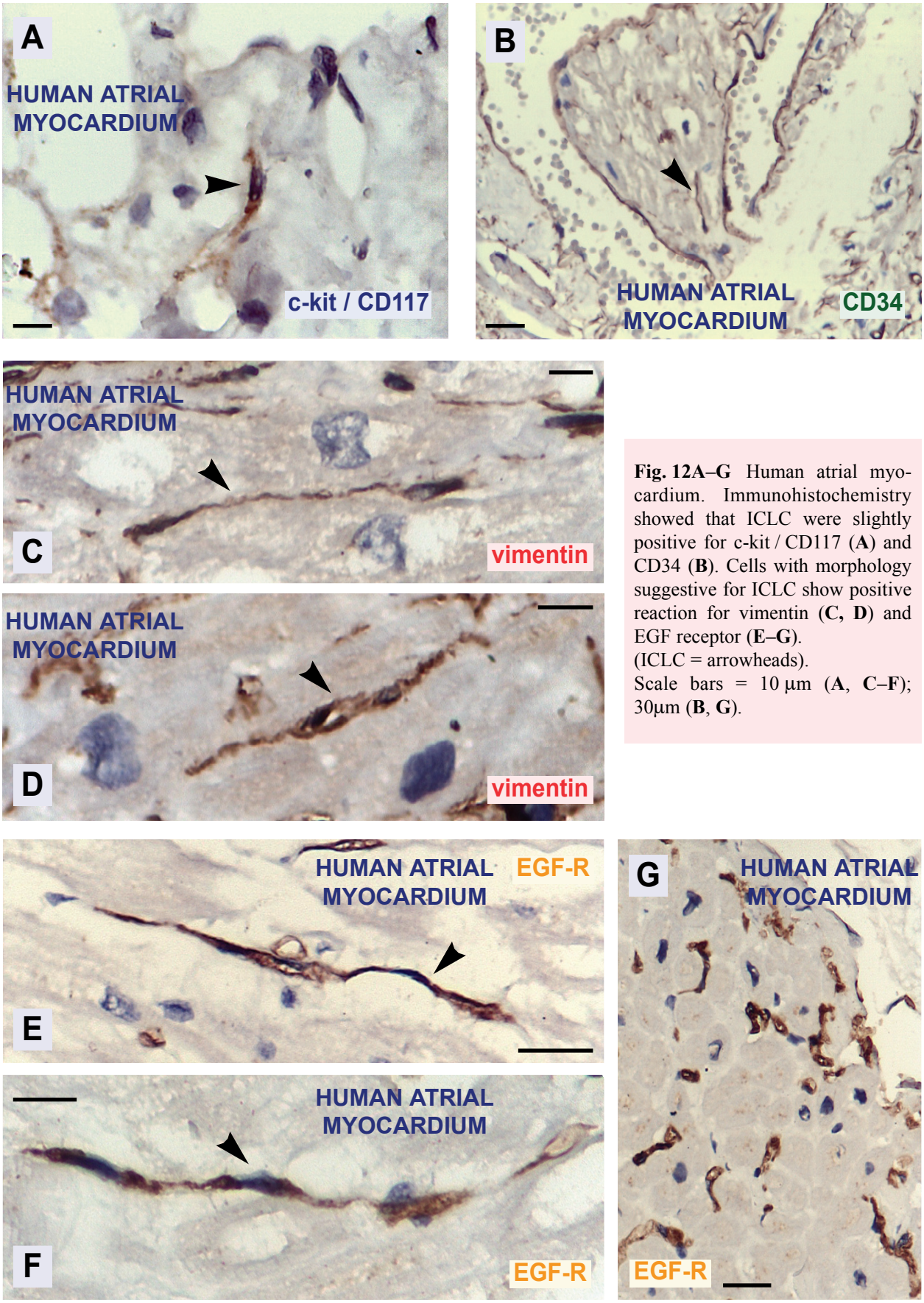

Fig. 12A–G Human atrial myocardium. Immunohistochemistry showed that ICLC were slightly positive for c-kit / CD117 (**A**) and CD34 (**B**). Cells with morphology suggestive for ICLC show positive reaction for vimentin (**C, D**) and EGF receptor (**E–G**).
(ICLC = arrowheads).
Scale bars = 10 µm (**A**, **C–F**); 30µm (**B**, **G**).

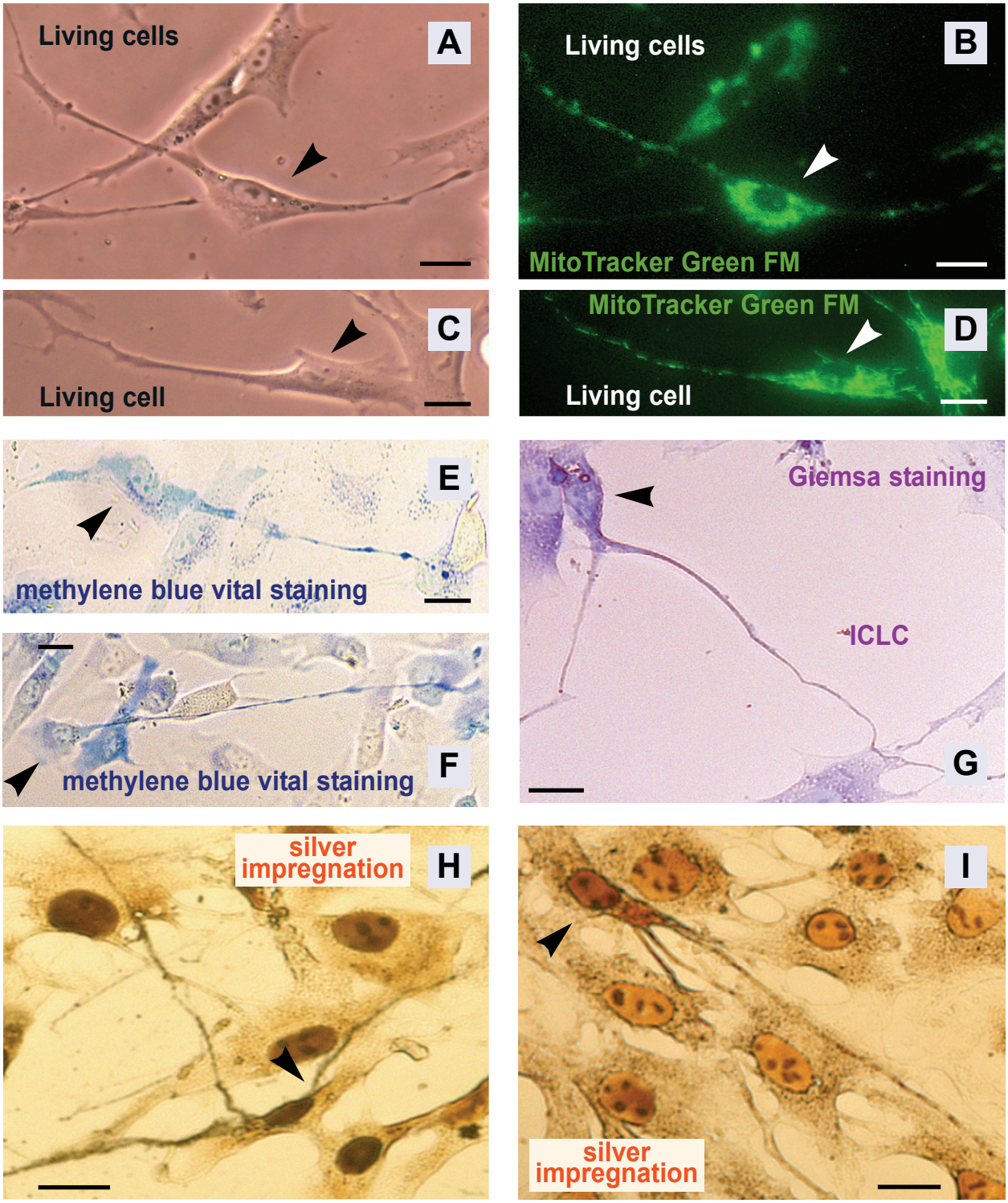

Fig. 13A–I Rat atrial myocardium. Interstitial Cajal-like cells (ICLC) isolated in preconfluent primary culture (day 4). **A**, **C**. Hoffman modulation contrast microscopy. **B**, **D**. The same cells as in **A**, **C** after vital staining with MitoTracker Green FM, a molecular probe for mitochondria. Observe the green fluorescent mitochondria in cell bodies and the typical moniliform ('beads on a string') appearance of cell prolongations. **E**, **F**. Methylene blue vital staining of ICLC. Note the selective staining of ICLC and the moniliform aspect of their processes. **G**. Giemsa staining. Two divergent, very thin cell processes. **H**, **I**. Silver impregnation reveals the delicate 'silhouette' of ICLC prolongations; note three and four such prolongations, respectively. arrowheads = ICLC. Scale bar = 10 μm.

into 24-well plates (BD Labware, San Jose,CA, USA) at a density of $1.5x10^4$ cells/cm^2, and maintained at 37°C, in a humidified atmosphere (5% CO_2 in air) until becoming semi-confluent (usually 4 days after plating).

The protocols used for *MitoTracker Green FM*, *methylene blue* and *Giemsa* stainings were previously described [13]. *Silver impregnation* on cell cultures was done as follows: cells were fixed with paraformaldehyde 2% for 10 min, at 4°C, washed 3 times in ethanol 80% and then incubated with silver nitrate 20%, for 30 min. Coverslips were then washed 3 times with water and covered with paraformaldehyde 20% for 3 min and then with amoniacal silver nitrate solution for 30 sec. Slides were then washed in distilled water, fixed in thiosulphate 5% and mounted in Entellan (Merck KGaA, Darmstadt, Germany).

Results

The toluidine blue staining of semi-thin sections from human atrium shows that ICLC are located among the working atrial myocytes. Figs. 1A–F & 2 reveal ICLC characteristic morphology: cell body shape and specific emerging cytoplasmic prolongations, which are very long and thin. Compare the characteristic aspects of cell processes in Figs. 1 & 2 with Fig. 13.

A strange morphological event is illustrated in Fig. 2. An extracellular lipid droplet (probably lipofuscin pigment) is surrounded by the ending of a long ICLC process. The presence of extracellular lipid material in myocardium has been previously documented [32].

Fig. 3 shows that about half of ICLC population has two prolongations per cell body, whilst only about 15% of ICLC have three cell processes.

In terms of relative volumes, ICLC seem to represent about 1.2±0.3% of the atrial myocardial volume vs. 44.9±2.9% working myocytes, 1.8±0.6% endothelial cells, 3.5±1.1 other interstitial cells, 48.6±2.5% extracellular matrix (Fig. 4).

Electron microscopy. TEM images obtained from both human and rat atrial ultrathin-sections have been digitally colored, in order to make ICLC (turquoise) more evident. Cells that were identified as ICLC fulfill ultrastructural criteria for positive diagnosis, proposed as an elegant 'gold standard' [33] and subsequently refined as 'platinum standard' [13]:

1. numerous mithochondria (Figs. 5B,C);
2. presence of intermediate filaments (Figs. 5B, 12);
3. absence of thick filaments (Figs. 5–11);
4. presence of surface caveolae (Figs. 7B–D, 8B,C); less than 1 / μm length of cell membrane;
5. variable basal lamina (Figs. 5B, 6);
6. close contacts between ICLC and nerve bundles (Figs. 7D, 8D, 9A,B);
7. presence of smooth and rough endoplasmic reticulum (Figs. 5A–C, 7A,C,D);
8. close apposition with target cells (Figs. 5A–C, 6, 8B–D);
9. specific target(s) in a given organ, e.g. for myocardium:
    a. working myocytes (Figs. 5A–C, 6, 7A,D, 8A–C, 9A–D), (average distance from ICLC: ~0.260±0.163 μm; n=98);
    b. nerve fibers (Figs. 7D, 8D), (distances from ICLC to nerve cells between 10.68 nm and 95.21 nm);
    c. capillaries (Figs. 7A–C, 8C, 9B, 10B,C), (average distance to endothelial cells: ~0.419±0.217 μm; n=34);
    d. other connective cells (e.g. macrophages). A multi-contact ('kiss and run') synapse with multiple, close-contact points (14 nm) alternating with wider intermembrane distances (36 to 92 nm) is presented in Fig. 11.
10. characteristic cell processes (Figs. 5–11):
    a. number - 1–3, frequently 2;
    b. length (tens of micrometers, usually 20–30μm);
    c. thickness (mean ~0.148±0.107 μm; n=54); (N.B.: close to the resolving power of the light microscope);
    d. their organization in network - labyrinthic system (overlapping cytoplasmic processes) or the dichotomous branching are noteworthy in Fig. 5A-C, 10A, 11.

Structures inside cardiomyocytes were (nearly) normal (Figs. 5A–C, 6–8, 9A,B), with little lipofuscin deposits (Fig. 6) and unevenly distributed atrial granules (Figs. 5A–C, 6, 7B,D, 8D, 9A,B, 10A,B).

IHC. The polyclonal antibodies used against CD117/c-kit resulted in weakly and inconstantly positive immunostaining of ICLC (Fig. 12A). Mast cells were also positive for CD117. The differential diagnosis was based on cell shape and prolongations (for ICLC) and the granular appearance (for mast cells). ICLC expressed CD34 antigen in

human atrial tissue specimens (Fig. 12B), and a network-like morphology was sometimes observed. However, CD34 alone may lead to an over-estimation of ICLC number, since CD34 might be expressed also by fibroblasts and endothelial cells. Vimentin was found strongly positive (Fig. 12C,D) along the ICLC cytoplasmic prolongations. Vimentin positive (c-kit negative) cells were found by Duquette *et al.* in pregnant human uterus [14] and considered such cells as being interstitial Cajal-like cells. We previously reported that c-kit positive cells, with ICLC morphology under the electron microscope, were present in human pregnant and non-pregnant myometrium [15].

Since the receptor for the epidermal growth factor (EGF-R) is considered the prototype for receptors with tyrosine kinase activity (related to c-kit receptor) and EGF-R is present on many cell types, we tested EGF-R expression by ICLC. (Un)expectedly, some atrial ICLC indeed appeared EGF-R positive (Fig. 12E–G).

ICLC were positive for α-smooth muscle actin and tau protein, and negative for nestin and S-100.

IHC for desmin showed the lack of expression at the level of ICLC, concomitantly with immunopositive reactions in working myocytes.

CD13 (Aminopeptidase N) is a transmembrane protease present in a wide variety of human cell types (endothelial, epithelial, fibroblast, leukocyte) and the negative immunoreaction that we found supported the differential diagnosis *vs.* classical fibroblasts [34].

In vitro, mitochondria retained the vital stain MitoTracker Green FM, corresponding with dilations of cytoplasmic processes, observed by Hoffman modulation contrast microscopy.

Typical ICLC (Fig. 13E,F) were easily recognized in cell culture using a vital dye: methylene blue. The selectively stained cells were designated as ICLC.

Similar result were obtained using Giemsa stain, since it is a mixture containing methylene-blue eosinate and methylene-blue chloride, dissolved in methyl alcohol, with glycerol as a stabiliser. Fig. 13G displays a spectacular ICLC.

Silver impregnation demonstrated specific staining of ICLC *in situ* [13] and we applied the same method to cells in culture. Indeed, ICLC with particular morphology (two or more very long, moniliform processes) stained selectively (Fig. 13H,I).

Discussion

This study provides further proof for the ICLC presence in human and rat atrial myocardium. To our knowledge, the existence of ICLC in the heart was overlooked until now. Table I presents [based on refs. 35–47] an incomplete survey of literature incidentally documenting (but ignoring) the occurence of ICLC or cell processes/fragments, in atrial myocardium. According to actual criteria for ultrastructural diagnosis [9, 13, 33], such cells can now be classified as putative ICLC.

Based on our algorythm for ICLC identification, the cells described in this study meet these criteria. The main issue might be that ICLC could be fibroblasts or myofibroblasts. Since 'fibroblasts are principally motile cells that contain actin (mainly α-smooth muscle actin) and myosin' [28], the absence of thick filaments does represent a pro-ICLC argument. Also, *in situ* ICLC have caveolae (while fibroblasts have caveolae only in cell culture), the level of development of rough endoplasmic reticulum (very abundant in fibroblasts), the presence of basal lamina, very ‘special’ cell processes etc., all these are additional arguments.

Noteworthy, myofibroblasts are 'not a typical component of normal untraumatised tissues' [48], although the structural remodeling of the myocardium (associated with mechanical overload or cardiac infarction) may be accompanied by the appearance of myofibroblasts [49]. Anyway, the ultrastructural obligatory criteria for myofibroblasts [50, 51] are not accomplished in the case of ‘our’ ICLC:

(i) stress fibers;
(ii) cell-to-stroma attachment sites (fibronexuses);
(iii) intercellular intermediate (adherens) and gap junctions.

The close plasmalemmal appositions that bring ICLC and macrophage together in a multicontact type stromal synapse, presented in Fig. 11, offers a signaling structural platform, being well within the molecular range [52]. We have previously identified stromal synapses in various organs (between ICLC and immunoreactive cells), supporting the hypothesis that stromal immunoreactive cells are included among the ICLC targets in interstitial intercellular communication.

Identification of ICLC confirms the belief that information made available by TEM is usually not

available by other approaches [53]. IHC may add value to TEM analysis.

Further investigation must be undertaken before presumptions about physiological significance (or lack of significance) of tau protein positivity in ICLC can be made.

Conventional and non-conventional light microscopy including immunocytochemistry are not enough for the positive diagnosis of ICLC, but are useful for quantitative data analysis, evaluation of relationships with target cells (working myocytes, nerve fibers, capillaries). Analysis of ultrastructural features by TEM still remains decisive for the positive diagnosis of ICLC.

Because of their position in interstitium, ICLC might be presumed as potential:

1) players in pacemaking, including arrhythmogenesis;
2) intermediates between intrinsic nerve fibres and myocytes (intercellular signaling);
3) a paracrine and/or juxtacrine source of signal molecules
4) mechanical transducers;
5) local 'triggers' for atrial granules content release;
6) tissue 'organizers' during development; uncommitted progenitor cells;
7) the 'neglected' component of tissue architecture during remodeling.

Instead of conclusion

Why ICLCs should not be the hearts of the heart?

Acknowledgments

The authors are grateful to Prof. Carmen Ardeleanu for expert assistance in IHC, to Dr. D. Cretoiu for his imagination in playing with images, to Dr. I. Droc, from the Center for Cardiovascular Disease, and to Ph.D. students Linda Cruceru, A. Popa, Antoanela Curici, Laura Caravia and Viviana Popa for their help. Also, the expert technical assistance of Mr. T. Regalia is gratefully acknowledged.

The authors thank Dr. B. Eyden, Manchester, for the useful comments on some electron micrographs.

References

1. **Komuro T, Seki K, Horiguchi K.** Ultrastructural characterization of the interstitial cells of Cajal. *Arch Histol Cytol.* 1999; 62:295-316.
2. **Rumessen JJ, Vanderwinden JM.** Interstitial cells in the musculature of the gastrointestinal tract: Cajal and beyond. *Int Rev Cytol*. 2003; 229:115-208.
3. **Faussone-Pellegrini MS.** Interstitial cells of Cajal: once negligible players, now blazing protagonists. *Ital J Anat Embryol*. 2005; 110:11-31.
4. **Hirota S, Isozaki K.** Pathology of gastrointestinal stromal tumors. *Pathol Int*. 2006;56:1-9.
5. **Faussone-Pellegrini MS.** Relationships between neurokinin receptor-expressing interstitial cells of Cajal and tachykininergic nerves in the gut. *J Cell Mol Med*. 2006; 10:20-32
6. **Hirst GD, Ward SM.** Interstitial cells: involvement in rhythmicity and neural control of gut smooth muscle. *J Physiol*. 2003; 550:337-46.
7. **Takaki M.** Gut pacemaker cells: the interstitial cells of Cajal (ICC). *J Smooth Muscle Res*. 2003; 39:137-61.
8. **Sanders KM, Koh SD, Ward SM.** Interstitial cells of cajal as pacemakers in the gastrointestinal tract. *Annu Rev Physiol*. 2006; 68:307-43.
9. **Huizinga JD, Faussone-Pellegrini MS**. About the presence of interstitial cells of Cajal outside the musculature of the gastrointestinal tract, *J Cell Mol Med.* 2005; 9:468-73
10. **Harhun MI, Pucovsky V, Povstyan OV, Gordienko DV, Bolton TB** Interstitial cells in the vasculature. *J Cell Mol Med* 2005; 9:232-43
11. **Bobryshev YV.** Subset of cells immunopositive for neurokinin-1 receptor identified as arterial interstitial cells of Cajal in human large arteries. *Cell Tissue Res*. 2005; 321:45-55.
12. **Popescu LM, Hinescu ME, Ionescu N, Ciontea SM, Cretoiu D, Ardeleanu C,** Interstitial cells of Cajal in pancreas. *J Cell Mol Med* 2005; 9:169-90
13. **Popescu LM, Ciontea SM, Cretoiu D, Hinescu ME, Radu E, Ionescu N, Ceausu M, Gherghiceanu M, Braga RI, Vasilescu F, Zagrean L, Ardeleanu C,** Novel type of interstitial cell (Cajal-like) in human fallopian tube. *J Cell Mol Med* 2005; 9:479-523
14. **Duquette RA, Shmygol A, Vaillant C, Mobasheri A, Pope M, Burdyga T, Wray S.** Vimentin-positive, c-kit-negative interstitial cells in human and rat uterus: a role in pacemaking? *Biol Reprod* 2005; 72:276-83
15. **Ciontea SM, Radu E, Regalia T, Ceafalan L, Cretoiu D, Gherghiceanu M, Braga RI, Malincenco M, Zagrean L, Hinescu ME Popescu LM,** C-kit immunopositive interstitial cells (Cajal-type) in human myometrium; *J Cell Mol Med* 2005; 9:407-20
16. **Van der Aa F, Roskams T, Blyweert W, De Ridder D.** Interstitial cells in the human prostate: a new therapeutic target? *Prostate*. 2003; 56: 250-5.
17. **Hashitani H, Suzuki H.** Identification of interstitial cells of Cajal in corporal tissues of the guinea-pig penis. *Br J Pharmacol*. 2004; 141: 199-204.

18. **Lang RJ, Klemm MF.** Interstitial cell of Cajal-like cells in the upper urinary tract. *J Cell Mol Med* 2005; 9:543-56
19. **Bradley E, Hollywood MA, McHale NG, Thornbury KD, Sergeant GP.** Pacemaker activity in urethral interstitial cells is not dependent on capacitative calcium entry. *Am J Physiol Cell Physiol*. 2005; 289:C625-32.
20. **Davidson RA, McCloskey KD.** Morphology and localization of interstitial cells in the guinea pig bladder: structural relationships with smooth muscle and neurons. *J Urol* 2005; 173:1385-90
21. **Brading AF.** Spontaneous activity of lower urinary tract smooth muscles: correlation between ion channels and tissue function. *J Physiol*. 2006; 570:13-22.
22. **Gherghiceanu M, Popescu LM.** Interstitial Cajal-like cells (ICLC) in human resting mammary gland stroma. Transmission electron microscopy identification *J Cell Mol Med* 2005; 9:893-910
23. **Bussolati G.** Of GISTs and EGISTs, ICCs and ICs. *Virchows Arch*. 2005; 447:907-8.
24. **Hinescu ME, Popescu LM,** Interstitial Cajal-like cells (ICLC) human atrial myocardium, *J Cell Mol Med* 2005; 9: 972-5
25. **Mudhar HS, Wagner BE, Suvarna SK**, Electron microscopy of myocardial tissue. A nine year review. *J Clin Pathol.* 2001; 54:321-5.
26. **Heinz D,** Quantitative ultrastructural data of animal and human cells, *Veb Georg Thieme* Leipzig, 1977
27. **Adler CP, Friedburg H, GW Herget, Neuburger M Schwalb H**, Variability of cardiomyocyte DNA content, ploidy level and nuclear number in mammalian hearts, *Virchows Arch* 1996; 429:159-64
28. **Camelliti P, Borg TK, Kohl P**. Structural and functional characterisation of cardiac fibroblasts. *Cardiovasc Res.* 2005; 65:40-51
29. **Weibel ER**. Practical methods for biological morphometry. Stereological methods. London: Academic Press, 1979
30. **Hsu SM, Rainel L, Fanger H,** Use of ABC und unlabeled antibody (PAP) procedures, *J Histoch Cytochem.* 1981; 29:577-580
31. **Bussolati G, Gugliotta P**: Nonspecific staining of mast cells by avidin – biotin – peroxidase complexes (ABC), *J Histochem Cytochem*, 1983; 31:1419-21
32. **Roy PE.** Lipid droplets in the heart interstitium: concentration and distribution. *Recent Adv Stud Cardiac Struct Metab*. 1975; 10:17-27.
33. **Huizinga JD, Thuneberg L, Vanderwinden J-M, Rumessen JJ.** Interstitial cells of Cajal as targets for pharmacological intervention in gastrointestinal motor disorders, *Trends Pharmacol Sci* 1997; 18:393–403
34. **Bauvois B, Dauzonne D.** Aminopeptidase-N/CD13 (EC 3.4.11.2) inhibitors: chemistry, biological evaluations, and therapeutic prospects. *Med Res Rev*. 2006; 26:88-130.
35. **Jamieson JD, Palade GE**, Specific granules in strial muscles. *J Cell Biol* 1964; 23:151-72
36. **Napolitano LM, Willman VL, Hanlon CR, Cooper T**., Intrinsic innervation of the heart. *Am J Physiol* 1965; 208:455-458
37. **James TN, Sherf L.,** Ultrastructure of the human atrioventricular node, *Circulation*, 1968; 37:1049-70
38. **McNutt NS, Fawcett DW**, The ultrastructure of the cat myocardium II. Atrial muscle, *J Cell Biol* 1969; 42:46-67
39. **Purdy JE, Liebeman M, Roggeveen AE, Kirk RG**. Synthetic strands of cardiac muscle. Formation and ultrastructure. *J Cell Biol* 1972; 55:563-78
40. **Viragh S, Challice CE**, Origin and differentiation of cardiac muscle cells in the mouse, *J Ultrastruct Res* 1973; 42:1-24
41. **Legato MJ.,** Ultrastructure of the atrial, ventricular, and Purkinje cell, with special reference to the genesis of arrhythmias, *Circulation*. 1973; 47:178-89.
42. **Denoit-Mazet F, Vassort G**. Ultrastructure des faisceaux sino-auriculaires de grenouille en relation avec leur activite electrophysiologique *J Microscopie (Paris)* 1971; 12:413-24
43. **Van der Zypen E**, On catecholamine-containing cells in the rat interatrial septum, *Cell Tissue Res* 1974; 151:201-18
44. **Nishi K, Yoshikawa Y, Sugahara K, Morioka T**, Changes in electrical activity and ultrastructure of sinoatrial nodal cells of the rabbit's heart exposed to hypoxic solution, *Circ Res*. 1980; 46:201-13
45. **Forsmann WG**, Morphological review: immunohistochemistry and ultrastructure of the endocrine heart, pp13-42, in: Forsmann WG, Scheuermann DW, Alt J (eds.), *Functional Morphology of the Endocrine Heart*, Springer Verlag, 1988
46. **Schramm E, Wagner M, Nellessen U, Inselmann G**, Ultrastructural changes of human cardiac atrial nerve endings in diabetes mellitus, *Eur J Clin Invest* 2000; 30: 311–6
47. **Rasmussen HB, Moller M, Knaus HG, Jensen BS, Olesen SP, Jorgensen NK**. Subcellular localization of the delayed rectifier K(+) channels KCNQ1 and ERG1 in the rat heart, *Am J Physiol Heart Circ Physiol*. 2004; 286:H1300-9
48. **Eyden B.** The myofibroblast: a study of normal, reactive and neoplastic tissues, with an emphasis on ultrastructure. Part 1—normal and reactive cells. *J Submicrosc Cytol Pathol*. 2005;37:109-204
49. **Miragoli M, Gaudesius G, Rohr S.** Electrotonic modulation of cardiac impulse conduction by myofibroblasts. *Circ Res*. 2006; [Epub ahead of print]
50. **Schurch W, Seemayer TA, Gabbiani G.** The myofibroblast: a quarter century after its discovery. *Am J Surg Pathol.* 1998; 22: 141-7.
51. **Eyden B.** The myofibroblast: an assessment of controversial issues and a definition useful in diagnosis and research. *Ultrastruct Pathol*. 2001; 25: 39-50.
52. **Popescu LM, Gherghiceanu M, Cretoiu D, Radu E.** The connective connection: interstitial cells of Cajal (ICC) and ICC-like cells establish synapses with immunoreactive cells. Electron microscope study in situ. *J Cell Mol Med* 2005; 9:714-30.
53. **Griffiths G**, Bringing electron microscopy back into focus for cell biology, *Trends Cell Biol* 2001; 11:153-154